RESEARCH ARTICLE | OCTOBER 26 2022

~8.5 μ m-emitting InP-based quantum cascade lasers grown on GaAs by metal-organic chemical vapor deposition Θ

S. Xu; S. Zhang [0]; J. D. Kirch [0]; S. Suri; N. Pokharel [0]; H. Gao; H. Kim [0]; P. Dhingra [0]; M. L. Lee [0]; D. Botez [0]; L. J. Mawst \square [0]

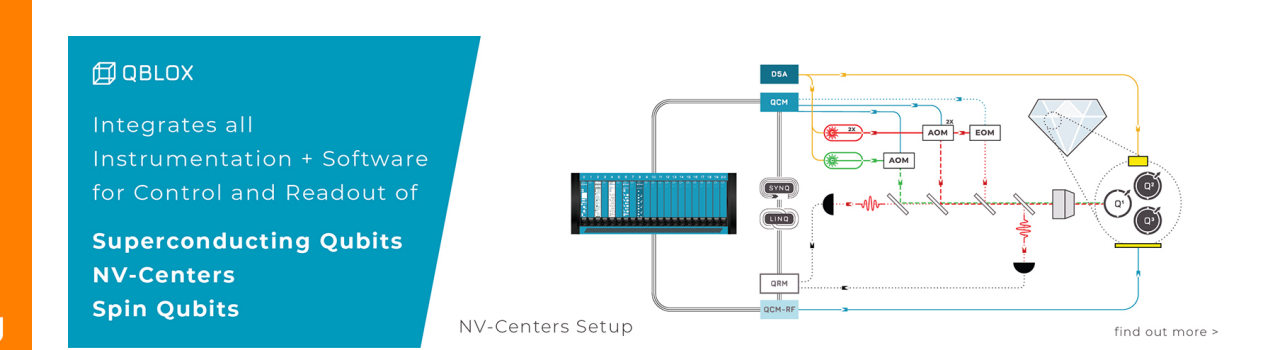


Appl. Phys. Lett. 121, 171103 (2022) https://doi.org/10.1063/5.0122272





CrossMark





\sim 8.5 μ m-emitting InP-based quantum cascade lasers grown on GaAs by metal-organic chemical vapor deposition

Cite as: Appl. Phys. Lett. **121**, 171103 (2022); doi: 10.1063/5.0122272 Submitted: 23 August 2022 · Accepted: 6 October 2022 · Published Online: 26 October 2022







S. Xu, S. Zhang, D. D. Kirch, S. Suri, N. Pokharel, D. H. Gao, H. Kim, D. P. Dhingra, D. M. L. Lee, D. Botez, D. and L. J. Mawst D.

AFFILIATIONS

- ¹Deparment of Electrical and Computer Engineering, University of Wisconsin, Madison, Wisconsin 53706, USA
- ²Department of Electrical and Computer Engineering, University of Illinois, Urbana-Champaign, Illinois 61801, USA

ABSTRACT

Room-temperature, pulsed-operation lasing of $8.5 \,\mu$ m-emitting InP-based quantum cascade lasers (QCLs), with low threshold-current density and watt-level output power, is demonstrated from structures grown on (001) GaAs substrates by metal-organic chemical vapor deposition. Prior to growing the laser structure, which contains a 35-stage In_{0.53}Ga_{0.47}As/In_{0.52}Al_{0.48}As lattice-matched active-core region, a \sim 2 μ m-thick nearly fully relaxed InP buffer with strained 1.6 nm-thick InAs quantum-dot-like dislocation-filter layers was grown. A smooth terminal buffer-layer surface, with roughness as low as 0.4 nm on a $10 \times 10 \,\mu$ m² scale, was obtained, while the estimated threading-dislocation density was in the mid-range \times 10⁸ cm⁻². A series of measurements, on lasers grown on InP metamorphic buffer layers (MBLs) and on native InP substrates, were performed for understanding the impact of the buffer-layer's surface roughness, residual strain, and threading-dislocation density on unipolar devices such as QCLs. As-cleaved devices, grown on InP MBLs, were fabricated as 25 μ m \times 3 mm deep-etched ridge guides with lateral current injection. The results are pulsed maximum output power of 1.95 W/facet and a low threshold-current density of 1.86 kA/cm² at 293 K. These values are comparable to those obtained from devices grown on InP: 2.09 W/facet and 2.42 kA/cm². This demonstrates the relative insensitivity of the device-performance metrics on high residual threading-dislocation density, and high-performance InP-based QCLs emitting near 8 μ m can be achieved on lattice-mismatched substrates.

Published under an exclusive license by AIP Publishing. https://doi.org/10.1063/5.0122272

Since its first demonstration in early 1990s, the quantum cascade laser (QCL) has achieved high-power continuous-wave (CW) operation and wide- and tunable wavelength in the mid-infrared (IR) and terahertz wavelength ranges, suitable for various applications, such as remote gas sensing, biomedical diagnosis, and free-space communication. To adapt the mature Si-based CMOS fabrication techniques and functionality of the optoelectronics platform developed in industry, direct integration by heteroepitaxy becomes appealing to achieve low cost, high-yield, and high-performance III–V semiconductor light sources on chip. Several wafer-bonding methods for III–V devices onto Si have been developed and demonstrated, but the limitations for such heterogenous integration are not negligible in terms of wafer size mismatch, precise waveguide alignment, and device reliability, therefore inhibiting large-scale production. 7–10

The growth of InP-based QCLs on GaAs (~4% lattice mismatch) is viewed as the intermediate first step toward realizing high

performance mid-IR lasers on Si, due to the large mismatch between InP and Si (\sim 8% lattice mismatch). To date, only a few monolithic QCLs on lattice-mismatched substrates have been demonstrated. Go et al.11 reported the first experimental demonstration of InGaAs/ InAlAs/InP QCLs grown on GaAs using an InAlAs compositionally graded buffer layer, achieving pulsed output powers of only a few tens of milliwatts at room temperature. More recently, Slivken and Razeghi¹² reported high peak-pulsed power (>10 W from both facets) InGaAs/InAlAs/InP QCLs grown on GaAs by employing a single InPbuffer layer, both devices emitted in mid-IR wavelength range $(4-5 \mu m)$, but suffered from high threshold-current densities, 4.1 and 3.4 kA/cm², much larger than those on native substrate, 1.3 and 1.4 kA/cm², respectively. The same InGaAs/InAlAs/InP QCL design on GaAs was later integrated onto a Si substrate, 6° miscut toward [111], with GaAs on Ge-terminated Si substrate as well as previous composite InAlAs buffer layer by Go et al.; 13 however, lasing was

^{a)}Author to whom correspondence should be addressed: ljmawst@wisc.edu

observed only up to 170 K. While these prior reports are promising, the underlying mechanisms responsible for performance degradation on lattice-mismatched substrates need further investigation.

Interestingly, longer wavelength (8–11 μ m) QCLs, consisting of binary InAs-based materials, have shown a high tolerance to dislocations, and the performance is close to that grown on a native substrate. 14,15 To date, all demonstrated QCLs' active-core regions have been grown by either solid-source or gas-source molecular beam epitaxy (MBE). Herein, we report the metalorganic chemical vapor deposition (MOCVD)-grown low-strain InGaAs/InAlAs/InP ~8 μm-emitting QCLs on GaAs substrate, which exhibit the lowest threshold current density reported for InGaAs/AlInAs/InP QCLs on lattice-mismatched substrate. In addition, these data demonstrate that the performance of InP-based QCLs employing "low-strain" ternary materials, such as InGaAs/InAlAs, is relatively immune to dislocations.

In this work, all material growths were carried out at 100 Torr within a vertical chamber (3 × 2 in. multi-wafer) MOCVD reactor, close-coupled showerhead (CCS) configuration, using H2 as a carrier gas, and TMIn, TMAl, TMGa, AsH₃, and PH₃ as precursors, and diluted disilane (Si₂H₆) as doping source. The metamorphic buffer layers (MBLs) employed a conventional two-step growth method on n-doped (001) GaAs substrate, with first growing a 70 nm-thick InP nucleation layer at 475 °C, and the chamber temperature was then raised to 650 °C under PH₃, and a 500 nm-thick high temperature InP layer was grown. Then, the chamber temperature was reduced to 480 °C where three repetitions of 1.6 nm InAs and 37 nm InP pairs were grown under abrupt AsH3 and PH3 gas switching at each interface. This process was repeated four times totally with 200 nm InP spacers in-between and a final 500 nm-thick InP top layer grown at 650 °C. The thermal cycling approach and strained dislocation filter layers (DFLs) were used to improve the overall buffer quality^{6,16,17} and are similar to the approach used for demonstrating 1.55 μ m-emitting quantum well diode lasers on mismatched GaAs substrate.¹

Then, native n-doped InP wafer and InP MBL template with 1.6 nm InAs DFLs were placed into the reactor for completing the laser structure growth at the same time. Before laser growth, a 300 nm-thick heavily doped In_{0.53}GaAs layer for lateral current injection and a 200 nm-thick intentionally un-doped InP layer were grown to avoid unnecessary current spreading into the n-doped InP substrate. The laser structure consists of a $2 \mu m$ -thick n-doped $(2 \times 10^{16} \, \text{cm}^{-3})$ lower InP cladding layer, followed by 300 nm-thick n-doped (5 \times 10¹⁶ cm⁻³) In_{0.53}GaAs optical confinement layers, with a 35-stage, lattice-matched to InP, In_{0.53}Ga_{0.47}As/In_{0.52}Al_{0.48}As QCL active region designed for \sim 8.2 μ m-emission using a two-phonon resonance design. 19 The injection layers in active region were doped to a target of $2 \times 10^{17} \, \mathrm{cm}^{-3}$. Then, a 3 $\mu \mathrm{m}$ -thick lightly doped (2×10^{16} cm⁻³) and a 500 nm-thick higher doped (2 \times 10¹⁷ cm⁻³) thick upper InP cladding were adopted for reducing plasmonic losses, followed by a heavily doped InP layer for metal contact. The wafers later were fabricated into 25 µm-wide and 3 mm-long deep etched ridge configuration, as shown in Fig. 1(a). Schematic representations of the completed laser structure on InP MBL are included in the supplementary material, Fig. S1, and the detailed fabrication procedure has been previously reported.

The InP MBL on GaAs with four-periods of three-repitition 1.6 nm InAs and 37 nm InP has root-mean-squared roughness value \sim 0.4 nm on 10 \times 10 μ m² scale, as measured by atomic force microscopy, and the threading dislocation density (TDD) was estimated to be in the mid-range \times 10⁸ cm⁻² by electron channeling contrast imaging (seen in the supplementary material, Fig. S2). The cross-sectional transmission electron microscopy (TEM) under (220) dark field view reveals that the dislocation filter layers appear to be quantum dot-like, and some stacking faults were also seen penetrating through the buffer to the top surface (seen in the supplementary material, Fig. S3). From symmetrical (004) and asymmetrical (-2-24) high-resolution x-ray diffraction (HRXRD) reciprocal spacing mappings, the relaxation degree of the InP buffer was measured to be as high as 97%.

Although threading dislocations and stacking faults were observed in the buffer layer region, a planar and defect-free QCL active region was observed in Fig. 1(b) by scanning transmission electron

(c) DF TEM

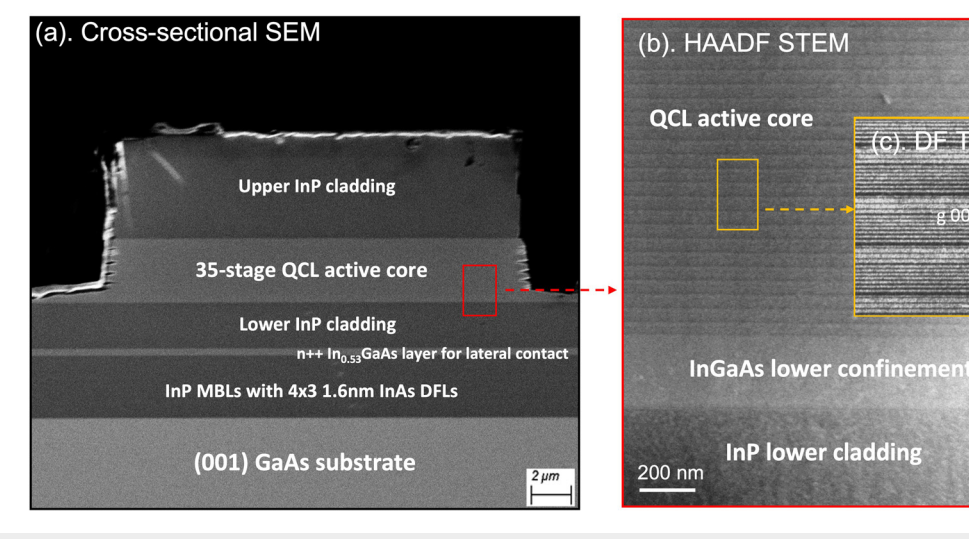


FIG. 1. Cross-sectional microscopy images of lattice matched 35-stage QCL on InP MBL with 4 imes 3 1.6 nm InAs DFLs. (a) Cross-sectional scanning electron microscopy (SEM), the ridge width is ~25 μ m, and interested layers are labeled; (b) high angle annular dark field (HAADF) scanning transmission electron microscopy (STEM) of active region. (c) Inset: finer resolution of a few stages of active region from (002) dark field transmission electron microscopy (DF-TEM).

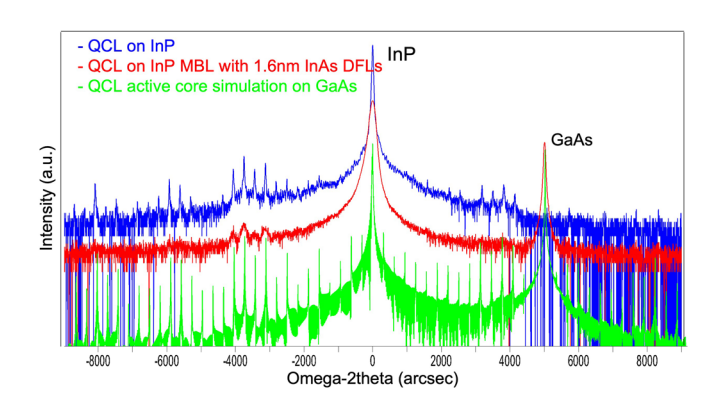


FIG. 2. Comparison of ω – 2θ measurements for completed laser structure with 35-stage In_{0.53}GaAs/In_{0.52}AlAs active region grown on InP and InP MBL on GaAs with simulation. The intensity is offset to see the satellite fringe peaks.

microscopy (STEM) under high-angle annular dark field (HAADF) conditions, within the sample's limited field of view. It is suspected that the lateral contact, lower cladding, and optical confinement layers grown below the QCL active core, providing additional thick buffer layers and helping with the migration of misfit dislocations to the edges. In addition, well-defined quantum wells and barriers with various thicknesses were observed from enlarged view by (002) dark field (DF) TEM in Fig. 1(c). Thus, a high structural quality of the laser core consisting of InGaAs/AlInAs materials lattice-matched to InP was achieved by MOCVD.

In contrast to our previous observation, for which a rapid reduction of the *in situ* reflectance occurred during the growth of a higherstrain QCL superlattice active region on a similar type of InP MBL, here only a slight reflectance reduction is observed during the last 5 stages of the "lattice-matched" active region for the growth on the MBL template, with well-defined *in situ* reflection interference fringes

were maintained during the entire laser growth. The lattice-matched materials in the laser core were chosen to avoid potential strain relaxation, which was expected to have occurred in our previous attempts at the growth of strain-compensated active region QCLs. The completed QCL structure grown on InP and MBL was then characterized by (004) HRXRD. The XRD fringes are broadened relative to the growth on InP substrate, as seen in Fig. 2, similar to a prior report of QCL on mismatched substrates. The XRD fringe broadening of QCL on InP MBL, compared with QCL on InP, may originate from the relatively high dislocation density, and the increased surface roughness after growing the thick laser structure on the MBL template. Development the x-ray diffraction peaks for the QCL core region grown on MBL are aligned well with those of the QCL core on InP and simulation.

As-cleaved devices with lateral top-side contacts were measured at room temperature under pulsed operation with a cavity length of 3 mm and ridge width of \sim 25 μ m. The threshold current density is 1.86 kA/cm² for the QCL on GaAs, surprisingly, values that are \sim 20% smaller than that of the QCL on InP, ~2.42 kA/cm². The maximum output power of QCLs on the MBL with 1.6 nm InAs DFLs was found to be \sim 1.95 W from one facet, which is comparable to that on InP, \sim 2.09 W per facet, even in the presence of relatively high residual MBL threading dislocation density, as shown in Fig. 3(a). We attribute this high performance in part to the use of a lattice-matched active region with a low roughness buffer layer, only 0.4 nm RMS roughness over $10 \times 10 \,\mu\text{m}^2$ area, as the roughness in the prior reports of InPbased QCLs on GaAs is significantly larger, 1.1 nm over $1 \times 1 \,\mu\text{m}^2$ area¹¹ and 1.2 nm over $10 \times 10 \,\mu\text{m}^2$ area, ¹² respectively. Similar insensitivity in device performance with respect to dislocation density was only observed previously in studies on (all-binary) InAs/GaSb/AlSb QCLs grown on lattice-mismatched substrates. 14,15 The 20% lower threshold current density and smaller dynamic range for the QCL devices on GaAs, compared to the counterpart on InP, might be related to reduced silicon dopant incorporation in the active region originating from the preexisting defects. Nevertheless, the 3 mm-long

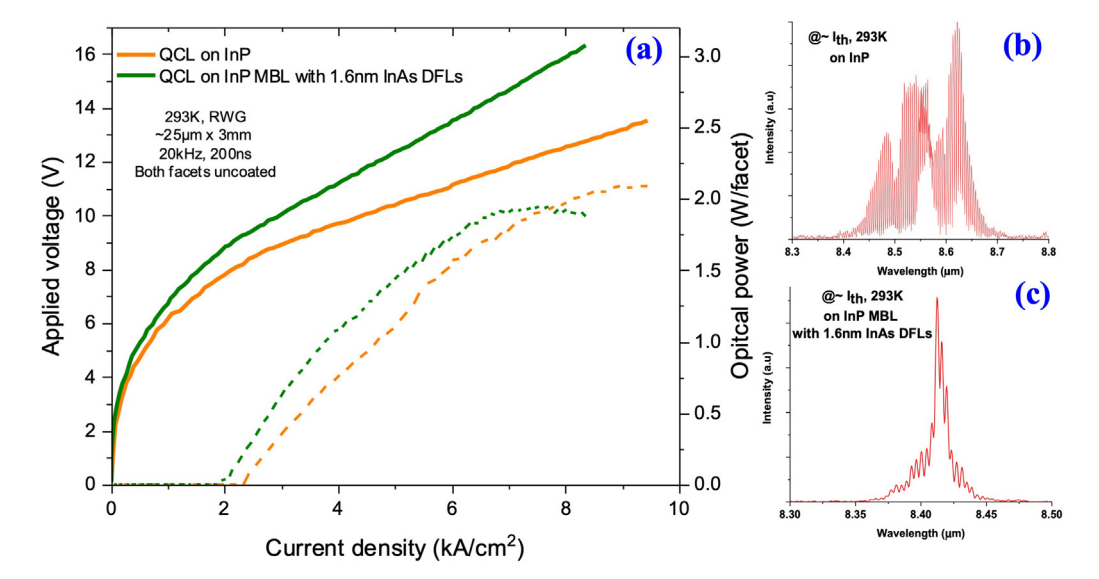


FIG. 3. (a) Characteristics of light power and applied voltage vs current density for \sim 25 μ m-wide and 3 mm-long uncoated ridge-guide devices on InP and on GaAs, at room temperature under pulsed operation. The right shows the lasing spectra for devices (b) on InP and (c) on InP MBL with 1.6 nm InAs DFLs around threshold current at RT.

uncoated devices on GaAs show slightly superior performance, compared to the counterpart on InP, in slope efficiency, 0.66 vs 0.56 W/A, and maximum wall-plug efficiency, 3.40% vs 3.05%. It should be also noted that the QCL devices on GaAs only have 4% higher turn-on voltage at threshold than the QCL on InP, but at least 20% higher voltage value at peak power, due to a higher series resistance. This may be related to non-uniform growth around defect sites, as indicated from the intensity reduction observed in the in situ reflectance measurement during MOCVD growth, which reduces the carrier mobility and tunneling efficiency locally, leading to a higher device series resistance. The lasing spectrum for QCL on GaAs is centered around 8.42 μ m, while for QCL on InP, it was red shifted to 8.55 μ m, at threshold conditions, seen in Figs. 3(b) and 3(c). This small emission wavelength shift might be due to the layer thickness variations or composition grading of the active core. Simulations indicate that the slight residual strain of the buffer layer is likely not the reason for the observed wavelength shift. The temperature dependence measurements were conducted, ranging from 20 to 60 °C, and then exponential fits were used to calculate the characteristic temperature coefficients for threshold current density (T₀) and slope efficiency (T₁) values. The extracted T₀ value is 218 K and T₁ value is 194 K for the QCL on GaAs, and the values for the QCL on InP are 172 and 410 K, respectively, which is comparable to prior reported characteristic temperature T₀ values (217 K) for this active region under pulsed operation. 19 Cavity-length studies were also performed on devices that were HR-coated on the back facet and cleaved to lengths varying between 2 and 4 mm; the internal loss for QCL on GaAs, extracted from a linear fit, is slightly higher than that on InP, 3.26 vs 2.76 cm⁻¹, and the internal quantum efficiency for the QCL on GaAs is also slightly higher, 26.2% vs 21.8%, although we expect that these differences may fall within the error bars of standard cavity length measurements.

In conclusion, we demonstrate the \sim 8 μ m-emitting InP-based quantum cascade laser monolithically integrated onto a (001) GaAs substrate by adapting strained InAs quantum-dot-like dislocation filter in InP buffers by MOCVD with low surface roughness. Similar device performance was achieved for QCL on GaAs compared to the counterpart on native InP substrate, with low threshold current density (1.86 kA/cm²) and high-output power (\sim 1.95 W/facet), in pulsed current operation at room temperature, from deep etched ridge-waveguide lasers with lateral current injection architecture. The achievement of high-performance ternary material QCL on GaAs also demonstrates the nature of the unipolar intersubband device's insensitivity to high dislocation density and provides insights into realizing QCLs on other non-native substrates, such as GaAs on Si.

See the supplementary material for the schematic representation of lattice-matched QCL laser structure on InP or InP MBL on GaAs and material characterization data.

The work at the University of Wisconsin-Madison was supported by the National Science Foundation (NSF ECCS No. 1806285).

AUTHOR DECLARATIONS Conflict of Interest

The authors have no conflicts to disclose.

Author Contributions

Shining Xu: Conceptualization (equal); Formal analysis (equal); Investigation (equal); Writing – original draft (equal). Dan Botez: Supervision (equal); Writing – review & editing (equal). Luke J. Mawst: Supervision (equal); Writing – review & editing (equal). Shuqi Zhang: Validation (equal). Jeremy Kirch: Conceptualization (equal). Suraj Suri: Investigation (supporting). Nikhil Pokharel: Investigation (equal). Huilong Gao: Investigation (supporting). Honghyuk Kim: Conceptualization (supporting). Pankul Dhingra: Investigation (equal). Minjoo Larry Lee: Supervision (supporting).

DATA AVAILABILITY

The data that support the findings of this study are available from the corresponding author upon reasonable request.

REFERENCES

- ¹V. M. Lavchiev and B. Jakoby, IEEE J. Sel. Top. Quantum Electron. 23, 452 (2017).
- ²N. Gayraud, Ł. W. Kornaszewski, J. M. Stone, J. C. Knight, D. T. Reid, D. P. Hand, and W. N. MacPherson, Appl. Opt. 47, 1269 (2008).
- ³O. Spitz, P. Didier, L. Durupt, D. A. Diaz-Thomas, A. N. Baranov, L. Cerutti, and F. Grillot, IEEE J. Sel. Top. Quantum Electron. 28, 1–9 (2022).
- ⁴Y. Han and K. M. Lau, J. Appl. Phys. **128**, 200901 (2020).
- ⁵E. Tournié, L. Monge Bartolome, M. Rio Calvo, Z. Loghmari, D. A. Díaz-Thomas, R. Teissier, A. N. Baranov, L. Cerutti, and J.-B. Rodriguez, Light: Sci. Appl. 11, 165 (2022).
- ⁶S. Chen, W. Li, J. Wu, Q. Jiang, M. Tang, S. Shutts, S. N. Elliott, A. Sobiesierski, A. J. Seeds, I. Ross, P. M. Smowton, and H. Liu, Nat. Photonics 10, 307 (2016).
- ⁷A. Spott, J. Peters, M. L. Davenport, E. J. Stanton, C. D. Merritt, W. W. Bewley, I. Vurgaftman, C. S. Kim, J. R. Meyer, J. Kirch, L. J. Mawst, D. Botez, and J. E. Bowers, Optica 3, 545 (2016).
- ⁸M. Tang, J.-S. Park, Z. Wang, S. Chen, P. Jurczak, A. Seeds, and H. Liu, Prog. Quantum Electron. 66, 1–18 (2019).
- ⁹G. Roelkens, J. Van Campenhout, J. Brouckaert, D. Van Thourhout, R. Baets, P. R. Romeo, P. Regreny, A. Kazmierczak, C. Seassal, X. Letartre, G. Hollinger, J. M. Fedeli, L. D. Cioccio, and C. Lagahe-Blanchard, Mater. Today 10, 36 (2007)
- 10 S. Stankovic, R. Jones, M. N. Sysak, J. M. Heck, G. Roelkens, and D. Van Thourhout, IEEE Photonics Technol. Lett. 24, 2155 (2012).
- ¹¹R. Go, H. Krysiak, M. Fetters, P. Figueiredo, M. Suttinger, J. Leshin, X. M. Fang, J. M. Fastenau, D. Lubyshev, A. W. K. Liu, A. Eisenbach, M. J. Furlong, and A. Lyakh, Appl. Phys. Lett. 112, 031103 (2018).
- ¹²S. Slivken and M. Razeghi, Photonics **9**, 231 (2022).
- ¹³R. Go, H. Krysiak, M. Fetters, P. Figueiredo, M. Suttinger, X. M. Fang, A. Eisenbach, J. M. Fastenau, D. Lubyshev, A. W. K. Liu, N. G. Huy, A. O. Morgan, S. A. Edwards, M. J. Furlong, and A. Lyakh, Opt. Express 26, 22389 (2018).
- ¹⁴H. Nguyen-Van, A. N. Baranov, Z. Loghmari, L. Cerutti, J.-B. Rodriguez, J. Tournet, G. Narcy, G. Boissier, G. Patriarche, M. Bahriz, E. Tournié, and R. Teissier, Sci. Rep. 8, 7206 (2018).
- ¹⁵Z. Loghmari, J.-B. Rodriguez, A. N. Baranov, M. Rio-Calvo, L. Cerutti, A. Meguekam, M. Bahriz, R. Teissier, and E. Tournié, APL Photonics 5, 041302 (2020).
- ¹⁶E. Delli, P. D. Hodgson, M. Bentley, E. Repiso, A. P. Craig, Q. Lu, R. Beanland, A. R. J. Marshall, A. Krier, and P. J. Carrington, Appl. Phys. Lett. 117, 131103 (2020).
- ¹⁷B. Shi and J. Klamkin, J. Appl. Phys. **127**, 033102 (2020).
- ¹⁸H. Kim, B. Shi, Z. Lingley, Q. Li, A. Rajeev, M. Brodie, K. M. Lau, T. F. Kuech, Y. Sin, and L. J. Mawst, Opt. Express 27, 33205 (2019).
- ¹⁹Z. Liu, D. Wasserman, S. S. Howard, A. J. Hoffman, C. F. Gmachl, X. Wang, T. Tanbun-Ek, L. Cheng, and F.-S. Choa, IEEE Photonics Technol. Lett. 18, 1347 (2006).
- ²⁰J. E. Ayers, J. Cryst. Growth **135**, 71 (1994).